LA-UR -81-3265

CONF-810839--4

TITLE: CALCULATION OF SCATTERING OF ELASTIC WAVES FROM FLAT CRACKS

AUTHOR(S): William M. Visscher, T-11

SUBMITTED TO: Proceedings of "AF/DARPA Review of Progress in Quantitative NDE"
Boulder, Colorado, August 1981

University of California

LOS ALAMOS SCIENTIFIC LABORATORY
Post Office Box 1663 Los Alamos, New Mexico 87545
An Affirmative Action/Equal Opportunity Employer

Form No. 836 R3
St. No. 2629
12/78

UNITED STATES
DEPARTMENT OF ENERGY
CONTRACT W-7405-ENG. 36

CALCULATION OF SCATTERING OF ELASTIC WAVES FROM FLAT CRACKS

William M. Visscher
Theoretical Division
Los Alamos National Laboratory
Los Alamos, NM 87545

ABSTRACT

A method, based on a boundary-integral representation of the elastic displacement, for calculating crack-opening-displacements on a flat crack of arbitrary shape and for incident elastic waves of arbitrary direction, polarization, and wavelength is developed and illustrated by application to Rayleigh scattering from two families of crack shapes. The crack-opening-displacement is expanded in a truncated complete set of functions on the crack surface. This transforms the boundary-integral representation into a matrix equation with rank three times the order of the truncation. This matrix equation has the properties that can be expressed as the result of an extremum principle with respect to variations of the expansion coefficients of the crack-opening-displacement (thus converges as the truncation order increases) and the matrix kernel (which must be inverted) is positive definite.

INTRODUCTION

Calculations of scattering from cracks in 3d are meager. Although geometrical diffraction theory can provide some results for very short wavelengths, there are in the literature no quantitative calculations of scattering from cracks of arbitrary shape at long or intermediate wavelengths.

Such a theory is here proposed and implemented. In the following we will develop the method and illustrate its application to flat cracks at long wavelength.

We start with an integral equation for the crack opening displacement, which is converted to a matrix equation by means of introducing a set of functions on the crack surface into which to expand the crack-opening-displacement (COD). The equation is solved for the COD in the Rayleigh limit, and results for scattering of long-wavelength elastic waves from two families of shapes of flat cracks are exhibited.

Integral Equation for the COD.

The equation with which we start is the surface-integral representation for the elastic displacement vector $\vec{u}(\vec{r})$. A convenient form is given by Boström and Kristensson[1]:

$$\vec{u}_{inc}(\vec{r}) + \frac{k_s}{\mu}\int_{S_1} d\vec{r}' \hat{n}\cdot\vec{\Sigma}(\vec{r},\vec{r}')\cdot\vec{u}(\vec{r}') = \begin{cases}\vec{u}(\vec{r}) & \vec{r}\in V_1 \\ 0 & \vec{r}\notin V_1\end{cases} . \quad (1)$$

Here S_1 is the boundary of a void as shown in Fig. 1. $\vec{\Sigma}$ is the Green's traction dyadic (several forms for it are given by BK), $\hat{n}$ is a unit vector normal to the surfaces, and $k_s^2 = \rho/\mu$, $k_l^2 = \rho/\lambda+2\mu$ are the wave numbers of shear and longitudinal waves propagating in a homogeneous and isotropic elastic medium with Lamé parameters λ, μ and density ρ. $\vec{u}_{inc}(\vec{r})$ is an incident plane wave.

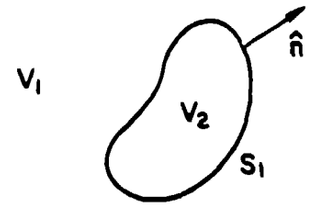

Fig. 1. The geometry associated with Eq. 1. The volume V_1 is filled with an elastic medium with Lamé parameters λ, μ and density ρ. V_2 is a void.

If the void becomes a crack, S_1 degenerates into a crack bottom and a crack top, both of which are the same open surface C_1. With the COD written as

$$\Delta\vec{u}(\vec{r}') = \vec{u}_{top}(\vec{r}') - \vec{u}_{bottom}(r') \quad , \quad (2)$$

Eq. (1) then takes the form, for $\vec{r}\in V_1$,

$$\vec{u}_{inc}(\vec{r}) + \frac{k_s}{\mu}\int_{C_1} dxdy\ \hat{n}\cdot\vec{\Sigma}(\vec{r},\vec{r}')\cdot\Delta\vec{u}(\vec{r}') = \vec{u}(\vec{r}) . \quad (3)$$

We have taken the crack to be flat, situated in the xy plane.

The traction dyadic $\hat{n}\cdot\vec{\Sigma}(\vec{r},\vec{r}')$ can be expressed in terms of the displacement dyadic $G(\vec{r},\vec{r}')$ which satisfies

$$C_{ijk\ell}G_{km,j\ell} + \rho\omega^2 G_{im} + (\mu/k_s)\delta_{im}\delta(\vec{r}-\vec{r}') = 0, \quad (4)$$

where the stiffness matrix is

$$C_{ijk\ell} = \lambda\,\delta_{ij}\delta_{k\ell} + \mu\,(\delta_{ik}\delta_{j\ell} + \delta_{i\ell}\delta_{jk}) \quad (5)$$

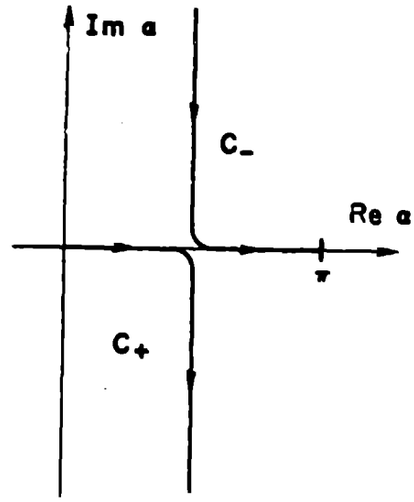

Fig. 2. The integration contours C_+ and C_-.

for an isotropic material[2] $G(\vec{r},\vec{r}')$ can be written in many equivalent forms; we find one given by BK to be most useful. It is

$$G_{ij}(\vec{r},\vec{r}') = 2i \int_{C^{\pm}} d\hat{\gamma}\, \phi_i^{\pi}(\hat{\gamma},\vec{r})\, \phi_j^{\dagger\pi}(\hat{\gamma},\vec{r}'), \quad z \gtrless z' \qquad (6)$$

and can be derived from the more familiar forms.[2,3] In Eq. (6) the integration is over a (complex) solid angle $d\hat{\gamma} = d\beta \sin\alpha d\alpha$, the integration limits for β are $0 \le \beta \le 2\pi$, and α follows the contours shown in Fig. 2. The basis vectors $\vec{\phi}^{\pi}$ are solutions of the elastic wave equation

$$C_{ijk\ell}\, \phi_{k,j\ell}^{\pi} + \rho\omega\, \phi_i^{\pi} = 0 \qquad (7)$$

corresponding to polarization π. They are

$\pi = 1$, SH wave:

$$\vec{\phi}^{1}(\hat{\gamma},\vec{r}) = \frac{i\hat{\beta}}{4\pi}\, e^{ik_s \hat{\gamma}\cdot\vec{r}} ,$$

$\pi = 2$, SV wave:

$$\vec{\phi}^{2}(\hat{\gamma},\vec{r}) = \frac{\hat{\alpha}}{4\pi}\, e^{ik_s \hat{\gamma}\cdot\vec{r}} , \qquad (8)$$

$\pi = 3$, P wave:

$$\vec{\phi}^{3}(\hat{\gamma},\vec{r}) = \left(\frac{k_p}{k_s}\right)^{3/2} \frac{i\hat{\gamma}}{4\pi}\, e^{ik_p \hat{\gamma}\cdot\vec{r}} ,$$

where the three unit vectors $\hat{\alpha},\hat{\beta},\hat{\gamma}$ have cartesian components

$$\hat{\beta} = (-\sin\beta,\ \cos\beta,\ 0)$$

$$\hat{\alpha} = (\cos\alpha\cos\beta,\ \cos\alpha\sin\beta,\ -\sin\alpha) \qquad (9)$$

$$\hat{\gamma} = (\sin\alpha\sin\beta,\ \sin\alpha\cos\beta,\ \cos\alpha) .$$

Notice that although $\hat{\alpha}\cdot\hat{\alpha} = \beta\cdot\beta = 1$ and $\hat{\alpha}\cdot\beta = \hat{\alpha}\cdot\hat{\gamma} = \beta\cdot\hat{\gamma} = 0$, the components of $\hat{\alpha}$ and $\hat{\gamma}$ are unbounded, because, according to Fig. 2, $\sin\alpha$ is real and positive ($0 \le \sin\alpha \le \infty$) while $\cos\alpha$ is imaginary the basis vectors $\vec{\phi}^{\pi}(\hat{\gamma},\vec{r})$ grow or decay exponentially in z. $\phi^{\dagger}$ in Eq. (6) is the function obtained by replacing i with -i in Eq. (8) where it explicitly occurs. In passing it should be noted that the α-integral diverges for $\vec{r} = \vec{r}'$, reflecting the singular behavior of G at that point. The individual terms in the sum over $\pi = 1,2,3$ also diverge for $z = z'$, but the sum converges. The divergences become worse for the traction dyadic that we actually use in the following, but the infinities alway. miraculously cancel in the polarization sum.

We now define basis stresses corresponding to the displacement vectors $\vec{\phi}^{\pi}(\hat{\gamma},\vec{r})$ according to

$$\sigma_{ij} = C_{ijk\ell}(\phi_{k,\ell} + \phi_{\ell,k})$$

$$= \lambda\delta_{ij}\, \vec{\nabla}\cdot\vec{\phi} + \mu(\phi_{i,j} + \phi_{i,j}) , \qquad (10)$$

and basis traction vectors for a surface parallel to the xy plane

$$t_i = \sigma_{ij}\, \hat{n}_j = \sigma_{i3} . \qquad (11)$$

In terms of these quantities the traction dyadic is

$$\left(\hat{n}\cdot\vec{\Sigma}(\vec{r},\vec{r}')\right)_{ij} = 2i \int_{C^{\pm}} d\hat{\gamma}\, \phi_i^{\pi}(\hat{\gamma},\vec{r})\, t_j^{\dagger\pi}(\gamma,\vec{r}') \qquad z \gtrless 0 \qquad (12)$$

which, when substituted into Eq. (3), will allow one to calculate the displacement $u(\vec{r})$ when one knows the COD. In order to calculate the COD we operate with the traction operator on Eq. (3), giving

$$t_i^{inc}(\vec{r}) + \frac{2ik_s}{\mu} \int_{C_1} dx'dy' \int_{C_{\pm}} d^{\pi}\hat{\gamma}\, t_i^{\pi}(\hat{\gamma},\vec{r}) \times t_j^{\dagger\pi}(\hat{\gamma},\vec{r}')\Delta u_j(\vec{r}') = t_i(\vec{r}) \qquad z \gtrless 0 \qquad (13)$$

If $\vec{r}$ is on C_1, then the boundary conditions require that the right-hand side vanishes.

An important observation is that $t_i^{inc}(\vec{r})$ is continuous across the crack. Therefore the second term in Eq. (13) is also continuous and we can use either C^+ or C^- when $z = 0$. We will find it convenient to use their average $C = \frac{1}{2}(C^+ + C^-)$; then the contributions of certain terms to the kernel will conveniently cancel.

With this replacement for the contour, Eq. (13) is equivalent to that given by BP. In order to mitigate the singularities of the kernel, however, they integrate by parts on $\vec{r}'$ and use the elastic wave equation to yield a more decorous integral equation at the expense of introducing derivatives of the COD. We will find that these complications, produced by the precautions prescribed by BR to palliate the pathology of the kernel, do not occur in the scheme we will describe.

The Matrix Equation.

Our method for solving Eq. (23) for $\Delta u_j(\vec{r})$ is as follows. First, we pick a convenient complete set of real functions on C_1; call them $v_n(\vec{r}) = v_n(x,y)$ with $x, y \in C_1$. Then expand

$$\Delta u_j(\vec{r}) = \sum_{n=1}^{N} c_j^n \, v_n(\vec{r}) \quad , \tag{14}$$

(for practical reasons, the set $\{v_n\}$ is always truncated to N members), multiply Eq. (13) by $v_m(\vec{r})$ and integrate over dxdy on C_1 with z = 0. Then it becomes

$$\int_{C_1} dxdy \; v_n(\vec{r}) t_i^{inc}(\vec{r}) + \frac{2ik_s}{\mu} \int_{\bar{C}} d\hat{\gamma} \; t_i^{\pi}(\hat{\gamma},n) \times c_j^n = 0 \quad , \tag{15}$$

where

$$t_i^{\pi}(\hat{\gamma},n) = \int_{C_1} dxdy \; v_n(\vec{r}) \; t_i^{\pi}(\hat{\gamma},\vec{r}) \quad . \tag{16}$$

Now expand t_i^{inc} in the basis stresses

$$t_i^{inc}(\vec{r}) = \int_{\bar{C}} d\hat{\gamma} \; t_i^{\pi}(\hat{\gamma},\vec{r}) \; t_{\pi}^{inc}(\hat{\gamma}) \tag{17}$$

(it can therefore, be either upgoing ($\hat{\gamma} \in C^+$) or downgoing ($\hat{\gamma} \in C^-$)); then Eq. (15) becomes

$$\int_{\bar{C}} d\hat{\gamma} \; t_i^{\pi}(\hat{\gamma},m) \; t_{\pi}^{inc}(\hat{\gamma}) + \frac{2ik_s}{\mu} \int_{\bar{C}} d\hat{\gamma} \; t_i^{\pi}(\hat{\gamma},m) \; t_j^{\dagger\pi}(\hat{\gamma},n) \times c_j^n = 0 \tag{18}$$

Since the incident traction is presumed to be known, we can take

$$t_{\pi}^{inc}(\hat{\gamma}) = \delta_{\pi\pi_o} \delta(\hat{\gamma}-\hat{\gamma}_o) \, a_{\pi_o} \quad ; \tag{19}$$

then Eq. (18) becomes

$$a_{\pi_o} \, t_i^{\pi_o}(\hat{\gamma}_o,m) + \frac{2ik_s}{\mu} Q_{i,m;j,n} \, c_j^n = 0 \tag{20}$$

which can be solved for the 3N-vector $\vec{c}$ by inverting the 3N x 3N matrix Q.

A valuable way of viewing Eq. (18) is as the result of minimizing

$$I = \int_{\bar{C}} d\hat{\gamma} \; (t_{\pi}^{inc}(\hat{\gamma}) + t_j^{\dagger\pi}(\hat{\gamma},n) d_j^n)(t_{\pi}^{\dagger inc}(\hat{\gamma}) + t_i^{\pi}(\hat{\gamma},m) d_i^{*m}) \tag{21}$$

with respect to variations in $d_i^{*m} = -\frac{2ik_s}{\mu} c_i^{*m}$. I.e.,

$$\frac{\partial I}{\partial d_i^{*m}} = 0 \tag{22}$$

is exactly Eq. (18). This fact can be made the basis of a proof of convergence of a sequence of truncations N, N + 1, N + 2, . . . in much the same way as it was done for MOOT.[4]

Another feature of the matrix Q is worth mentioning. This is that at least in the long-wavelength limit it can be shown to have the form of the product of a non-singular matrix with its own hermitian conjugate. Such a matrix is positive-definite; this means that solving for the COD in this case is a well-posed problem and many kinds of numerical difficulties are, therefore, guaranteed not to occur.

The Q-Matrix.

The matrix Q defined by Eqs. (18) and (20) is

$$Q_{im;jn} = \int_{\bar{C}} d\hat{\gamma} \; t_i^{\pi}(\hat{\gamma},m) t_j^{\dagger\pi}(\hat{\gamma},n) = \int_{\bar{C}} d\hat{\gamma} \; w^{\pi}(\hat{\gamma},m) \, A_{ij}^{\pi} \, w^{\pi *}(\hat{\gamma},n) \quad , \tag{23}$$

where

$$w_n^{\pi}(\hat{\gamma}) = \int_{C_1} dxdy \; e^{ik_{\pi}\hat{\gamma}\cdot\vec{r}} \; v_n(\vec{r}) \quad , \tag{24}$$

and $k_{\pi} = k_s (\pi = 1,2)$, $k_{\pi} = k_p (\pi = 3)$, so A is just the product of derivatives (Eq. 10) of ϕ's (Eq. 8) without exponential factors.

Some simplications can be made immediately. First, notice that $w^{\pi}(\hat{\gamma},n)$ is the same on C^+ as on C^-; thus any terms in A which change sign between C^+ and C^- won't contribute to Q. The (13) and (23) terms in A have this behavior, so Q, for a given (n,m) pair, is block-diagonal. The z-COD does not mix with the x,y-CODs, in agreement with the results of BR.

Now we need to choose the complete set $v_n(\vec{r})$, n=1,2...N. The ideal set would allow us to perform the integral over C_1 in Eq. (24) analytically, and the integrals over β and α in Eq. (23) analytically also. The closest we have been able to come to this ideal is the set of gaussians

$$v_n(\vec{r}) = \frac{1}{2\pi\sigma^2} \exp(-(\vec{r}-\vec{r}_n)^2/2\sigma^2) \tag{25}$$

on the crack surface. The set of positions $\vec{r}_n = (x_n,y_n,0)$ can be chosen in some sort of regular array on C_1; by choosing the grid sufficiently fine (with the gaussian range σ appropriately small), it is easy to show that in the distribution sense v_n is complete.

With this choice of v_n, we have

$$w_n^{\pi}(\hat{\gamma}) = e^{ik_\pi \hat{\gamma}\cdot\vec{r}_n} e^{-(\sigma k_\pi \sin\alpha)^2/2} , \qquad (26)$$

which has a simple enough dependence on α and β to allow us to hope to do the integrals in Eq. (23) analytically. The integral over β yields regular Bessel functions of order 0 and 2. The integrals over α, however, must be computed numerically except in the long-wavelength limit ($k_\pi\sigma \to 0$), in which case they are expressible in terms of modified Bessel functions $I_{0,1}$.

The Q-matrix elements (Eq. (23)) are then

$$Q_{11} = \frac{3\lambda+4\mu}{\lambda+2\mu} S_o^2 - \cos 2\phi \frac{\lambda}{\lambda+2\mu} S_2^2$$

$$Q_{22} = \frac{3\lambda+4\mu}{\lambda+2\mu} S_o^2 + \cos 2\phi \frac{\lambda}{\lambda+2\mu} S_2^2$$

$$Q_{12} = - \frac{\lambda}{\lambda+2\mu} \sin 2\phi \, S_2^2$$

$$Q_{33} = 4\frac{\lambda+\mu}{\lambda+2\mu} S_o^2 , \qquad (27)$$

where a common factor $\mu^2/16\pi\kappa\sigma^2$ has been omitted, and

$$S_o^2 = (i\sqrt{\pi}/2)e^{-x}[(\tfrac{1}{2}-x)I_o(x) + xI_1(x)]$$

$$S_2^2 = (i\sqrt{\pi}/2)e^{-x}[xI_o(x) - (x+\tfrac{1}{2})I_1(x)] .$$

Each of Eqs. (27) are N x N matrices (the n, m indices have been suppressed): $\phi = \phi_{nm} = \arctan(y_n - y_m / x_n - x_m)$, $x = \rho^2/8$, $\rho = r_{nm}/\sigma$. So Q is a $3N_n \times 3N_m$ block-diagonal matrix with one N x N block and one 2N x 2N block.

The fact that the Q-matrix elements are pure imaginary combines with the i in Eq. (20) to insure that the COD will be in phase with the incident stress, as must be the case in this limit.

The gaussian basis functions $v_n(\vec{r})$ need to be specified. For simplicity and versatility we have taken $\vec{r}_n$ to form a regular 2d lattice, either square or triangular depending on the problem, with lattice spacing a determined by the crack size and shape. The only parameter then remaining arbitrary is σ, the gaussian range.

As long as $\sigma \leq a$ and a is sufficiently small relative to the crack size, results should be insensitive to σ, since the completeness criterion we need to fulfill can be satisfied as well as we like. But in practice, of course, we can't let a be arbitrarily small, because we need to compute and invert the Q-matrix. For the present we have used only a 7 x 7 array of basis functions, so 2N = 98 at most.

What we have chosen to do[**] to fix σ is to pick a crack for which an exact solution is known, namely, the penny-shaped (circular) crack, simulate its CODs with an arrays of gaussians, and vary σ until our calculated average CODs match the exact average CODs.

Long wavelength scattering from a circular crack in the xy plane can be parametrized by two quantities; namely, the average z-COD produced by an asymptotic traction in the z-direction, and by the average x (or y)-COD produced by an asymptotic traction in the x (or y)-direction. The ratio of these quantities (x-COD)/(z-COD) = R depends only on Poisson's ratio in the exact calculation; in ours it depends also on σ. For Poisson's ratio = $\lambda/2(\lambda+\mu) = 1/3$, it happens that R = 6/5.[5] For the arrays shown in Fig. 3, which are our simulations of circular cracks, we can reproduce R = 6/5 if $\sigma = 0.376$ for the hexagonal approximation to the circle and if $\sigma = 0.398$ for the octagonal one.[#] The z-COD itself depends on the magnitude of the asymptotic z-traction and on the radius of the penny-shaped crack; by requiring that our computed average z-COD using the just-determined σ equal the exact average COD, one can deduce the radius; this is how the circles in Fig. 3 were drawn.

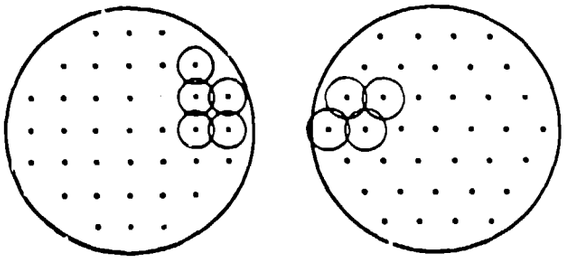

(a) (b)

Fig. 3. Arrays $\vec{r}_n$ of centers for basis functions. The circles are the edges of the penny-shaped cracks whose Rayleigh scattering is exactly reproduced by our calculations using the pictured arrays, which are our simulations of penny-shaped cracks using square (a) and triangular (b) arrays. This requirement of matching exact results fixes $\sigma = 0.398$ in (a), and $\sigma = 0.376$ in (b). The small circles delineate the 1/e range ($= \sqrt{2}\sigma$) of the basis gaussians.

The singularity in the COD at the crack edge (COD $\sim\sqrt{R^2-r^2}$) is not accurately described in our simulation. The edge singularity is important if one wishes to estimate stress-intensity factors, but not scattering cross-sections, because the latter can be expressed[6] in terms of the Fourier transforms of the COD with $k = k_\pi$. As long as the scale of our errors is small compared to a wavelength our computed cross-sections will be right.

Scattering from Flat Cracks of Arbitrary Shape.

The matrix equation [Eq. (20)] is most useful when applied to non-circular cracks, which have not been computed by any other method. To illustrate the procedure, we will in this section calculate Rayleigh scattering from two families of crack shapes.

It has been shown[7] that long-wavelength scattering from flat cracks can be parametrized with six real numbers. Three of these are orientation angles, one is a scale parameter which is determined by the crack size, and two are fixed

by the crack shape. Therefore a two-parameter family of shapes generally exhausts all possible scattering signatures.

Starting with a square crack, one family can be generated by cutting out a rectangle from its center; the two shape parameters are then the ratios of the sides of the rectangle to the side of the square. This we will call the O-family. Another family can be generated by making a corner of the omitted rectangle coincident with the corner of the square. This is the L-family.

The three parameters (one scale parameter and two shape parameters) are in correspondence with three of the parameters A_{ijkl} of Ref. 7, in terms of which the scattering can be naturally expressed. To a common multiplier, A_{1313} is the average COD in the ith direction caused by an asymptotic strain in the jth direction. One can always rotate the crack in its plane (the xy plane) so that $A_{1323} = A_{2313} = 0$, leaving only A_{3333}, A_{1313}, and A_{2323} to parametrize the scattering. The forward (and back)-scattered longitudinal amplitude for a normally-incident longitudinal wave is proportional to A_{3333}; in Ref. 7 are defined

$$\beta = \frac{1}{2}(A_{1313} + A_{2323})/A_{3333}$$
$$\gamma_o = \frac{1}{2}(A_{1313} - A_{2323})/A_{3333} \qquad (28)$$

which depend only on the crack shape. These number pairs should be in one-to-one correspondence with our two shape parameters. This correspondence is illustrated in Fig. 4 for the O-family and in Fig. 5 for the L-family. We have taken

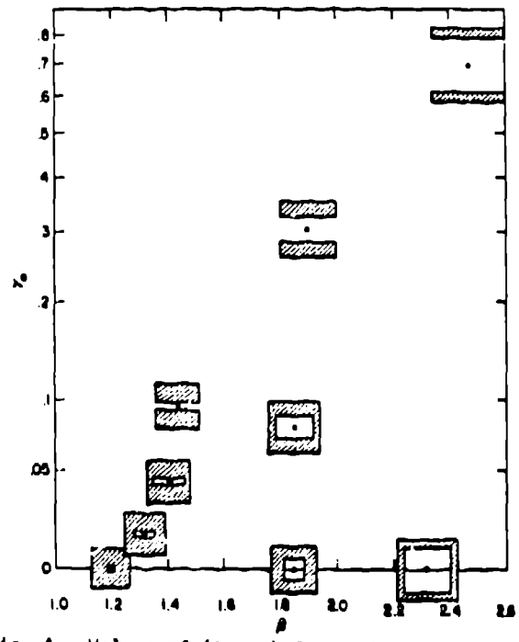

Fig. 4. Values of (β, γ_o) for members of the O-family of crack shapes. The relative sizes of the illustrated cracks are adjusted so that all have equal A_{3333}. The numbers for the more extreme members, such as the two parallel rectangular cracks each with aspect ratio 7:1 should not be trusted quantitatively because they are represented by 7 x 1 arrays of basis functions.

the various members of the two families represented them with a portion of a 7 x 7 square array of gaussian basis functions, and obtained the CODs by solving Eq. (20). From the CODs we obtain β and γ_o from Eq. (28) and plot a point on Fig. 7 or 8. The crack is then drawn at that point; its orientation is adjusted so that $A_{1323} = 0$ and its size is adjusted so that all the cracks illustrated have equal A_{3333}, hence equal normally incident longitudinal-longitudinal backscattering. It appears that to each accessible point (β, γ_o) on Figs. 4 and 5 (the upper left portion appears to be physically unrealizable) there corresponds a set of shape parameters for the O-family and for the L-family. Since Rayleigh scattering depends only on β, γ_o, and A_{3333} this means that an O-crack cannot be distinguished from an L-crack with the same (β, γ_o). The same can be said of an infinite number of other shape families.

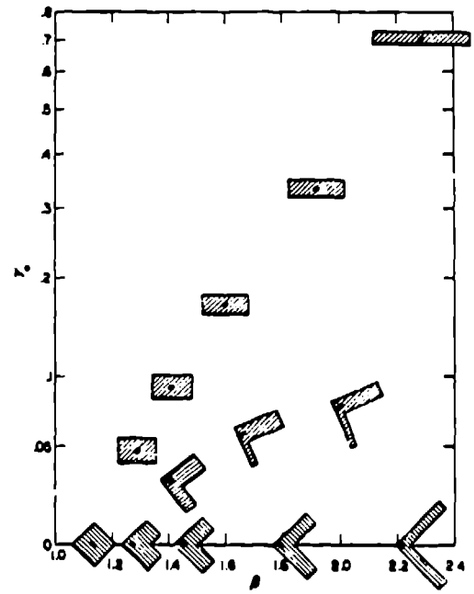

Fig. 5. Values of (β, γ_o) for members of the L-family of crack shapes. Sizes are adjusted so that all cracks here and in Fig. 4 have the same longitudinal backscattering of a normally incident longitudinal wave. Orientation is such that $A_{1323} = 0$. Cracks appearing at the same (β, γ_o) on this plot and on Fig. 4 are indistinguishable to long-wavelength elastic waves.

Summary.

Starting from a boundary-integral representation for the elastic displacement, we have computed the CODs in the Rayleigh limit for a variety of planar crack shapes, and have shown how to compute them for higher frequencies for planar cracks of general shape.

The key steps in the development were:

1) Selection of the appropriate expansion of the Green's dyadic. This allowed one to deduce a matrix equation which has a positive definite kernel and is derivable from an extremum principle.

2) Expansion of the CODs in a complete set of functions on the crack surface. This formed the basis for the matrix equation mentioned above.

3) Felicitous choice of this set of expansion functions, which allows the development to proceed as far as possible before consigning it to the computer.

Acknowledgement

This work was supported by the US DOE-BES contract E412.

References

1. A. Boström and G. Kristensson, "Elastic Wave Scattering by a Three-Dimensional Inhomogeneity in an Elastic Half-Space," Wave Motion 2 335-353 (1980) (Referred to in text as BK).

2. For references see J. E. Gubernatis, E. Domany, and J. A. Krumhansl, "Elastic Wave Scattering Theory with Application to Nondestructive Evaluation," in Physical Principles of Non-Destructive Evaluation, ed. D. O. Thompson (Springer-Verlag, to be published).

3. B. Budiansky and J. R. Rice, "An Integral Equation for Dynamic Response of an Isolated 3-D Crack," Wave Motion 1 187-192 (1979) (Referred to in text as BR).

4. William M. Visscher, "A New Way to Calculate Scattering of Acoustic and Elastic Waves. I. Theory Illustrated for Scalar Waves," J. Appl. Phys. 51 825-834 (1980); "... II. Application to Elastic Waves Scattering From Voids and Fixed Rigid Obstacles," J. Appl. Phys. 51 835-845 (1980).

5. S. Teitel, "Quasistatic Approximation to the Scattering of an Arbitrarily Incident Elastic Plane Wave by an Elliptical Crack," J. Appl. Phys. (in press).

6. J. E. Gubernatis and E. Domany, "Rayleigh Scattering of Elastic Waves from Cracks," J. Appl. Phys. 50 810-824 (1979).

7. William M. Visscher, "Scattering of Elastic Waves from Planar Cracks in Isotropic Media," J. Acoust. Soc. Am. 69 50-53 (1981).

Footnotes

** One might think that, since Eq. (18) is the condition for I [Eq. (21)] to be an extreme with respect to variations in d_m^*, that the optimal σ could also be found variationally. This would be so if I were a boundary residual, as in the case of MOOT[4].

If σ is increased by 1%, R increases by about 2%.

This report is an abbreviated version of a paper to be published in Wave Motion.